J Mater Sci (2008) 43:6116–6121
DOI 10.1007/s10853-008-2940-3

Reaction-sintering of lead-free piezoceramic compositions: $(0.95 - x)Na_{0.5}K_{0.5}NbO_3$–$0.05LiTaO_3$–$xLiSbO_3$

Pornsuda Bomlai · Sureewan Sukprasert · Supasarote Muensit · Steven J. Milne

Received: 30 May 2008 / Accepted: 7 August 2008 / Published online: 4 September 2008

Abstract Incorporation of $LiSbO_3$ into the lead-free piezoceramic composition $0.95Na_{0.5}K_{0.5}NbO_3$–$0.05LiTaO_3$ produced a change from an orthorhombic to tetragonal crystal system in samples produced by reaction-sintering. The inferred limit of solid solution along the compositional join, $(0.95 - x)Na_{0.5}K_{0.5}NbO_3$–$0.05LiTaO_3$–$xLiSbO_3$, occurred at $x \sim 0.06$. Differential scanning calorimetry indicated broad peaks at temperatures associated with ferroelectric–paraelectric transitions. The transition temperatures decreased with increasing values of x, up to $x = 0.06$. Microstructures showed secondary grain growth; a slight decrease in grain-size with increasing $LiSbO_3$ modification was identified.

Introduction

Environmental concerns are stimulating research into the development of lead-free alternative piezoelectric ceramics [1, 2]. Mixed alkali niobate-tantalates are leading candidates as replacements for lead zirconate titanate, PZT.

P. Bomlai (✉) · S. Sukprasert
Materials Science Program, Faculty of Science, Prince of Songkla University, Songkhla 90112, Thailand
e-mail: ppornsuda@yahoo.com

S. Muensit
Department of Physics, Faculty of Science, Prince of Songkla University, Songkhla 90112, Thailand

S. J. Milne
Institute for Materials Research, University of Leeds, Leeds LS2 9JT, UK
e-mail: s.j.milne@leeds.ac.uk

Guo et al. [3] investigated the alkali niobate solid solution system $[Na_{0.5}K_{0.5}NbO_3]_{1-x}$–$[LiTaO_3]_x$ (abbreviated, NKN–LT) and reported a morphotropic phase boundary (MPB), at $0.05 < x < 0.06$, between orthorhombic and tetragonal phase fields. Compositions close to this MPB gave the highest values of d_{33} piezoelectric charge coefficients in the system, reaching a value of $\sim$200 pC/N at $x = 0.05$ with a corresponding Curie temperature (T_c) of $\sim$420 °C.

Saito et al. [4, 5] studied a wider range of related solid solutions, corresponding to the general formula $(K_{0.5}Na_{0.5})_{1-x}Li_xNb_{1-y}Ta_yO_3$. For a composition $x = 0.03$ and $y = 0.2$, close to the MPB of this system, $d_{33} = 230$ pC/N, with a T_c of 323 °C. Reactive template grain growth resulted in enhanced piezoelectric properties, giving values of $d_{33} = 373$ pC/N and $T_c = 323$ °C for ⟨001⟩ grain-oriented ceramics. Slightly improved values of d_{33} coefficients were obtained using Sb ion doping on the pentavalent sites of the perovskite lattice. These values approach those of some PZT ceramics and consequently have aroused keen interest in developing this compositional system further as a viable Pb-free piezoceramic [6–11].

Although the highest piezoelectric coefficients were demonstrated for textured ceramics fabricated using reactive template grain growth, these fabrication procedures are rather complicated and would be costly for commercial production. Hence it is important to optimize properties in conventional, randomly orientated ceramic samples. For example, Marcos et al. [12] have used conventional ceramic processing techniques to fabricate ceramics of $(K_{0.44}Na_{0.52}Li_{0.04})(Nb_{0.86}Ta_{0.10}Sb_{0.04})O_3$, and also a 'non-stoichiometric' composition $(K_{0.38}Na_{0.52}Li_{0.04})(Nb_{0.86}Ta_{0.10}Sb_{0.04})O_{2.97}$ [4]. A higher piezoelectric coefficient was obtained for the latter, with $d_{33} \sim 200$ pC/N.

There are still uncertainties regarding the precise compositional range of solid-solution formation in

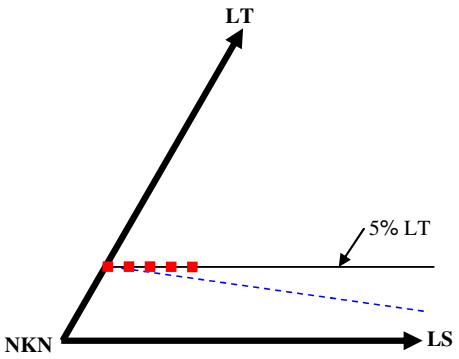

Fig. 1 Schematic showing location of compositional system, $(0.95 - x)Na_{0.5}K_{0.5}NbO_3$–$0.05LiTaO_3$–$xLiSbO_3$ (solid line marked by squares) in the NKN–LT–LS ternary system. For comparison, the binary join studied previously, $1 - x[0.95Na_{0.5}K_{0.5}NbO_3$–$0.05LiTaO_3]$–$xLiSbO_3$ is shown by a dashed line [12]

Sb-modified alkali niobates. The present paper reports the findings of a study of phase formation and microstructures of ceramic compositions along the unreported compositional join, $(0.95 - x)Na_{0.5}K_{0.5}NbO_3$–$0.05LiTaO_3$–$xLiSbO_3$, corresponding to the elemental formula $Na_{0.475-x}K_{0.475-x}Li_{0.05+x}(Nb_{0.95-x}Sb_xTa_{0.05})Sb_xO_3$. The position of this series in the NKN–LT–LS ternary system is shown in Fig. 1. To minimize losses of volatile components during ceramic fabrication, a reaction-sintering method was employed.

Experimental procedure

Samples were prepared by the conventional mixed-oxide process using K_2CO_3, Ta_2O_5 (Aldrich Chemical Company, Inc., ≥99.0% purity), Na_2CO_3, Nb_2O_5 (Aldrich Chemical Company, Inc., 99.9+% purity), Li_2CO_3 (Fluka, >99.0% purity), and Sb_2O_5 (Aldrich Chemical Company, Inc., 99.995% purity), as starting powders. Firstly the $Na_{0.5}K_{0.5}NbO_3$ powder was prepared. The two carbonate powders are moisture sensitive; thermogravimetric analysis indicates that dehydration is completed at ~200 °C. Therefore to avoid compositional errors when weighing out the $Na_{0.5}K_{0.5}NbO_3$ precursor mixture, the starting reagents were dried in an oven for 24 h prior to use. Dried powders were allowed to cool to room temperature under reduced pressure in a desiccator, and all powders were stored in the desiccator until immediately prior to weighing in the correct proportions. The starting materials were transferred to a 100 mm diameter cylindrical plastic jar, partially filled with 10 mm diameter alumina grinding balls. Sufficient ethanol was added to just cover the powder and grinding media. Ball milling was carried out for 24 h, followed by drying at 120 °C, prior to grinding with an alumina mortar and pestle to break up large agglomerates formed during drying. The mixtures were calcined in alumina crucibles, with loosely fitting lids, at 800 °C for 2 h. For reaction-sintering, the NKN powders were ground, weighed, and ball-milled again for 24 h with Ta_2O_5 and the volatile Li_2CO_3 and Sb_2O_5 components to obtain the compositions $(0.95 - x)Na_{0.5}K_{0.5}NbO_3$–$0.05LiTaO_3$–$xLiSbO_3$ (abbreviated as NKN–LT–LS) for $x = 0.0$, 0.02, 0.04, 0.06, and 0.10. No second powder calcination stage was employed prior to sintering. The mixed powders were dried, ground, and pressed at 100 MPa into 1.5 cm diameter discs and sintered in air at temperatures of 1050 °C and 1075 °C for 2 h in closed crucibles.

Ceramic samples were examined at room temperature using X-ray powder diffraction (XRD; Philips X' Pert MPD, Ni-filtered CuK_α radiation) to identify the phase(s) formed. No mechanical grinding or polishing was carried out prior to XRD. Sintered pellet densities were obtained by the Archimedes method. The density of ground pellets was determined by liquid displacement pycnometry using dry toluene; this enabled sintered pellet density to be expressed as a percentage value. The microstructures of the as-sintered surfaces of the samples were imaged directly, using scanning electron microscopy (SEM; Jeol: JSM-5800LV). The average grain size was calculated by the mean linear intercept method. Differential scanning calorimetry (PerkinElmer, DSC7) was carried out in a N_2 atmosphere at a heating rate of 10 °C/min.

Results and discussion

XRD patterns of ceramics of $(0.95 - x)Na_{0.5}K_{0.5}NbO_3$–$0.05LiTaO_3$–$xLiSbO_3$ compositions $x = 0$–0.1 are presented in Fig. 2. The intensity ratio of the pair of peaks at 45–46.5°2θ in each pattern was used as an indication of the tetragonal/orthorhombic phase content [13]. The lower angle peak in the pair corresponds to the 022 peak of an orthorhombic NKN–LT phase, or the 002 peak for tetragonal-phase NKN–LT [14, 15]. The neighbouring higher angle peak corresponds to the orthorhombic 002 peak, or the 200 peak of tetragonal NKN–LT. For orthorhombic NKN–LT, the peak intensity ratio, I_{022}/I_{002} is ~1.5–1.8; the precise value in this range depends on fabrication conditions, and possibly the level of volatilization losses [13, 16]. For a tetragonal, single phase NKN–LT pattern the corresponding ratio, I_{002}/I_{200} is ~0.5 [13]. The reported phase boundary between orthorhombic and tetragonal phases on the NKN–LT binary occurs around 6 mol% LT [3]. Hence the orthorhombic phase is the expected phase for the $x = 0$ composition, NKN–5 mol% LT, studied here [3]. The peak intensity ratios for all the $(0.95 - x)Na_{0.5}K_{0.5}NbO_3$–$0.05LiTaO_3$–$xLiSbO_3$ samples are shown in Table 1. The $x = 0$ composition had a peak intensity ratio of ~1.7 for the 1075 °C sample, Table 1, confirming it to be orthorhombic

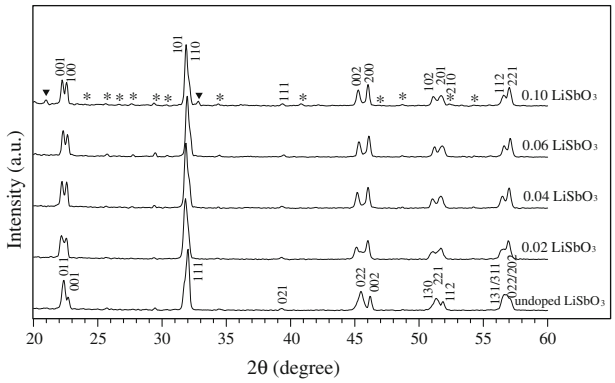

Fig. 2 XRD patterns of samples $(0.95 - x)[Na_{0.5}K_{0.5}NbO_3–0.05 LiTaO_3]–xLiSbO_3$ sintered at 1050 °C for 2 h (* = $K_6Li_4Nb_{10}O_{30}$ [18]; ▼ = $LiSbO_3$ [17])

Table 1 XRD data showing *d*-spacings and intensity ratios as a function of *x* (the mole fraction of $LiSbO_3$) and reaction-sintering temperatures

$LiSbO_3$ content, *x*	Sintering temperature (°C)	*d*-spacings (Å)		I_{022}/I_{002}	I_{002}/I_{200}
		022/002	002/200		
0.00	1050	1.994	1.966	1.38	–
	1075	2.003	1.971	1.69	–
0.02	1050	2.010	1.972	–	0.62
	1075	2.014	1.975	–	0.56
0.04	1050	2.006	1.972	–	0.78
	1075	2.011	1.974	–	0.58
0.06	1050	2.002	1.969	–	0.71
	1075	2.005	1.973	–	0.56
0.10	1050	2.004	1.972	–	0.72
	1075	2.004	1.973	–	0.48

NKN–LT [13]. However, the values of peak intensity ratio of all the Sb-modified samples, reaction-sintered at 1075 °C, were around 0.5, close to the value expected for a tetragonal NKN–LT perovskite solid solution. This change in crystal system, from orthorhombic to tetragonal, infers that solid solution formation has occurred as a result of reaction with the $LiSbO_3$ component. However there was no significant change in *d*-spacing over this range of compositions *x*, Table 1. Second-phase $LiSbO_3$ was detected in the $x = 0.1$ samples, Fig. 2, inferring a limit of LKN–LT–LS tetragonal solid solution around $x = 0.06$ [17].

The peak intensity ratios were slightly higher (~0.6–0.8) for samples sintered at the lower temperature of 1050 °C, which probably indicates that some orthorhombic phase was present, along with the main tetragonal phase. All samples showed faint XRD peaks due to a tungsten bronze phase [18] which has also been reported for various compositions along the binary NKN–LT join [3].

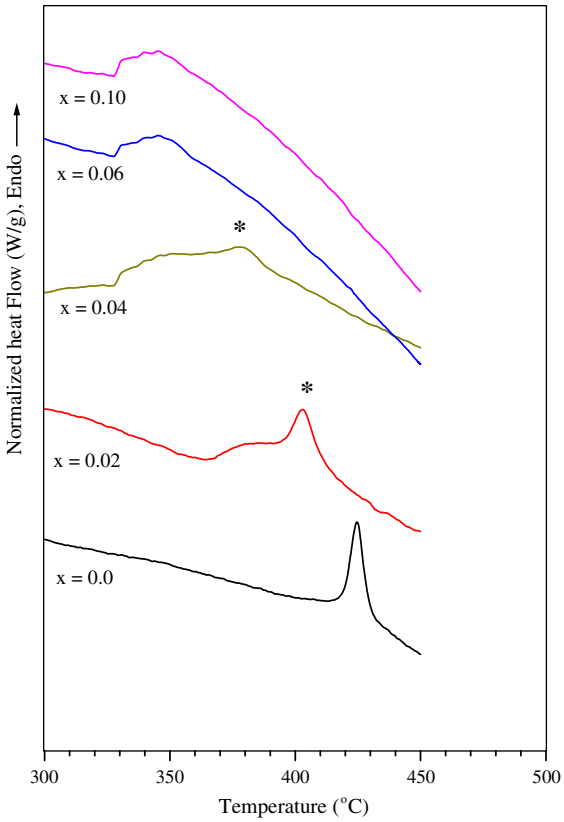

Fig. 3 DSC results of samples $(0.95 - x)Na_{0.5}K_{0.5}NbO_3–0.05 LiTaO_3–xLiSbO_3$ sintered at 1075 °C for 2 h. Asterisks indicate peaks thought to relate closely to the $0.95Na_{0.5}K_{0.5}NbO_3–0.05LiTaO_3$ end member—see text for details

DSC experiments revealed an endothermic peak for the $x = 0$ sample at a temperature of 425 °C, Fig. 3. This temperature is consistent with the reported value for the ferroelectric–paraelectric phase transition for binary NKN–LT compositions [3]. The DSC peak temperatures as a function of composition are summarized in Table 2. For the $x = 0.02$ sample an endotherm, made up of a distinct peak at 403 °C and an overlapping, much more diffuse peak centered around 385 °C (onset ~365 °C) was observed, Fig. 3. For sample $x = 0.04$, the DSC profile had similarities to the $x = 0.02$ sample, but the broader endotherm was relatively more intense and occurred at a lower temperature ~360 °C (onset 340 °C): a decrease in the temperature of the sharper peak, from 403 °C to 378 °C, also occurred. For the $x = 0.06$ and 0.1 compositions, only one broad endotherm was observed, centered at 346 °C (onset 328 °C).

The DSC data infer that two distinct types of solid solution exist in the $x = 0.02$ and 0.04 samples; peak broadening suggests the phases are each compositionally non-uniform. The sharper DSC peak in the $x = 0.02$ and $x = 0.04$ Sb-modified samples (marked by an asterisk on Fig. 3) appears to correlate to the ferroelectric–paraelectric

Table 2 Peak temperature from DSC analysis with various $LiSbO_3$ contents, x: two peaks could be distinguished in $x = 0.02$ and 0.04

$LiSbO_3$ content, x (mole)	Estimated peak temperature (°C)	
0.0	425	–
0.02	403	385(broad)
0.04	378	360 (broad)
0.06	–	346 (broad)
0.10	–	346 (broad)

(tetragonal–cubic) peak of the unmodified NKN–LT phase. The change in peak temperatures in $x = 0$–$x = 0.06$ is consistent with modification of the crystal lattice by substitution of Li and Sb ions. The similarity in DSC data between $x = 0.06$ and 0.01 suggests that the limit of Li SbO_3 solid solution occurs at $x \sim 0.06$, which is in agreement with the limit inferred from XRD data.

Reasons for the existence of two phases in the $x = 0.02$ and 0.04 samples are not fully understood. Based on the experimental XRD and DSC data it seems plausible that two distinct tetragonal solid solution phases, differing in average composition and transition temperature, are formed for $x = 0.02$ and 0.04. The phase giving rise to the broadest DSC peaks is presumed to approximate most closely to the desired product composition. Broadening points to local variations in ion ratio within each phase. The question arises as to why only a single, but very broad, peak exists for $x = 0.06$ (and 0.1). Liquid formation is very likely in this system given the low melting point of the Sb_2O_5 component (380 °C), and the lack of full powder calcination prior to sintering. An increase in the Sb_2O_5 content (in $x = 0.06$ and 0.1) would be expected to give an increase in the volume of liquid present, and contribute to higher reactivity, resulting in only one product phase.

Support for the premise of inhomogeneity in the samples is found in literature reports of related binary NKN–LT ceramics made by conventional processing (i.e. not involving reaction-sintering) in which SEM-EDX revealed the presence of severe compositional fluctuations [19]. The inhomogeneity could not be eliminated by prolonged high-temperature annealing [19]. Thus it seems that the broad, and in some cases double DSC peaks in the present samples are a consequence of compositional variability within the sample. XRD showed little evidence of peak broadening (Fig. 2), but our previous study into phase development during conventional powder calcination of NKN–LT indicated that d-spacings in such systems were insensitive to small changes in phase composition [13]. Here it is demonstrated that DSC is more sensitive than XRD in probing compositional homogeneity in lead-free alkali niobate piezoceramics.

Marcos et al. [12] reported that the formation of a solid solution along the more commonly studied join, $1 - x[0.95(Na,K)NbO_3$–$0.05LiTaO_3]$–$xLiSbO_3$, (indicated by a dashed line in Fig. 1) is extremely difficult to achieve due to the crystal structural differences between $KNbO_3$ and $NaNbO_3$, with perovskite crystal structures, and $LiTaO_3$ with a hexagonal pseudo-ilmenite crystal structure. However there are a number of reports into solid solution formation of related compositional series: for example $(1 - x)K_{0.5}Na_{0.5}(Nb_{0.925}Ta_{0.075})O_3$–$xLiSbO_3$ $(0 \leq x \leq 0.1)$ and also $(K_{0.44}Na_{0.52}Li_{0.04})$ $(Nb_{0.86}Ta_{0.10}Sb_{0.04})O_3$ [12, 20]. The results of conventional mixed oxide reactions for these compositions reveal that Li^+ and Sb^{5+} diffuse into the parent lattices to form a solid solution with a perovskite structure [20]. It is reported to be an orthorhombic phase at $x \leq 0.02$ and tetragonal at $x \geq 0.04$. Co-existence of the orthorhombic and tetragonal phases is found at $0.02 < x < 0.04$. The present XRD results for reaction-sintering at 1075 °C infer only tetragonal phase for the join $(0.95 - x)Na_{0.5}K_{0.5}NbO_3$–$0.05LiTaO_3$–$xLiSbO_3$. Although sintering at a lower temperature, 1050 °C leads to co-existence of tetragonal and orthorhombic phases, based on XRD peak intensity ratios (Table 1). A comprehensive study of the NKN–LT–LS section of the phase diagram would be required to determine the full extent of the compositional area of solid solution formation in this region.

In terms of the ceramic processing characteristics, there was little variation in density with increasing values of x, Fig. 4. A maximum density of 4.4 g/cm^3 at 1050 °C corresponded to ~92% of the value of powder density (4.78 g/cm^3). The slight decrease in sintered pellet density between 1050 °C and 1075 °C, Fig. 4, is most probably due to the effects of loss of volatile oxides. The sintering temperatures are close to the melting temperature; sintering at 1150 °C resulted in major changes to phase composition, with the appearance of a cubic phase inferring that partial melting and subsequent crystallization had occurred.

All compositions, $x = 0.02$–0.1, showed secondary recrystallization (secondary grain growth) after reaction-sintering at 1075 °C, Fig. 5. With increasing $LiSbO_3$

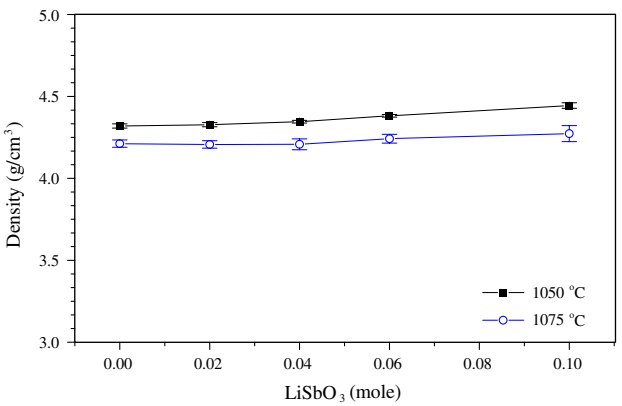

Fig. 4 The density values of samples $(0.95 - x)[Na_{0.5}K_{0.5}NbO_3$–$0.05LiTaO_3]$–$xLiSbO_3$ when reaction-sintered at different temperatures

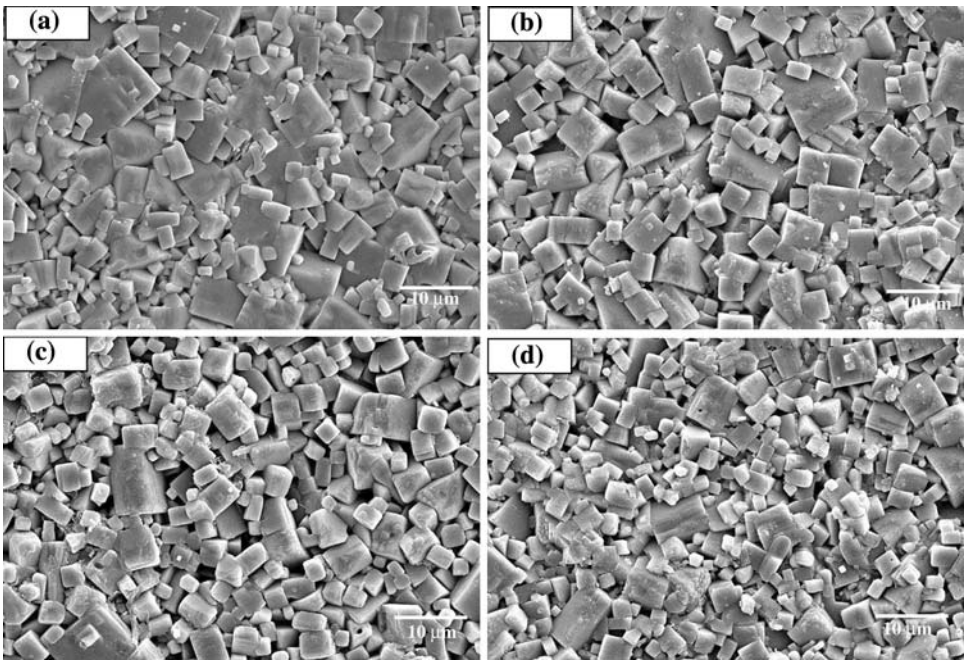

Fig. 5 SEM micrographs $(0.95 - x)[Na_{0.5}K_{0.5}NbO_3–0.05LiTaO_3]–xLiSbO_3$ samples where x is: (**a**) 0; (**b**) 0.02; (**c**) 0.04 and (**d**) 0.10 reaction-sintered at 1075 °C for 2 h

modification, there was a reduction in the fraction of secondary grains. The resulting variation in average grain size is shown in Fig. 6. In other perovskites such as $BaTiO_3$, secondary grain growth is often associated with liquid phase formation. A similar mechanism leading to bimodal grain size distributions is probable in the NKN–LT–LS system. For samples sintered at 1050 °C, secondary grain growth occurred only in the $x = 0.04$–0.1 compositions, inferring that insufficient liquid was present in $x < 0.04$ samples at this lower temperature to induce secondary recrystallization (Fig. 6).

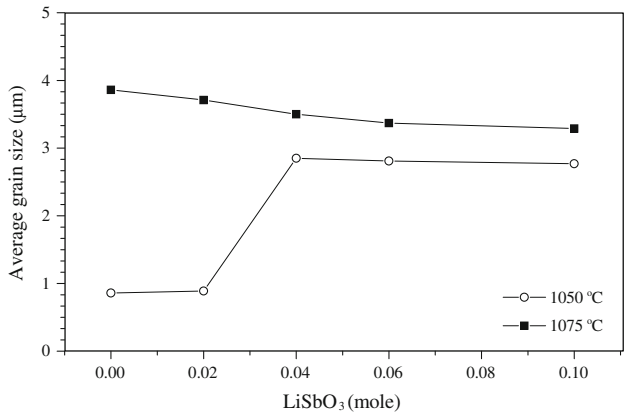

Fig. 6 Average grain size of $(0.95 - x)Na_{0.5}K_{0.5}NbO_3–0.05LiTaO_3–xLiSbO_3$ samples reaction-sintered at 1050 °C and 1075 °C for 2 h

Conclusions

Ceramics were produced by reaction-sintering of pre-calcined powders of $Na_{0.5}K_{0.5}NbO_3$ with Li_2CO_3, Ta_2O_5 and Sb_2O_5 powders, according to the formula, $(0.95 - x)Na_{0.5}K_{0.5}NbO_3–0.05LiTaO_3–xLiSbO_3$. Solid solution with $LiSbO_3$ induced a change from orthorhombic to tetragonal crystal system. Broad phase transition peaks were observed in DSC plots, suggesting significant levels of chemical inhomogeneity. The limit of solid solution is estimated to occur at $x \sim 0.06$. The maximum sintered pellet densities were around 92%.

Acknowledgements This work was supported by Thailand Research Fund (TRF) and Commission on Higher Education.

References

1. European Council (2003) Official Journal of the European Union L37:19
2. IEEE (1987) IEEE Standard on piezoelectricity, ANSI/IEEE standard no. 176 IEEE, New York
3. Guo Y, Kakimoto K, Ohsato H (2005) Mater Lett 59:241. doi:10.1016/j.matlet.2004.07.057
4. Saito Y, Takao H, Tani I, Nonoyama T, Takatori K, Homma T, Nagaya T, Nakamura M (2004) Nature 432:84. doi:10.1038/nature03028
5. Saito Y, Takao H (2006) Ferroelectrics 338:17. doi:10.1080/00150190600732512
6. Zuo R, Rödel J, Chen R, Li L (2006) J Am Ceram Soc 89:2010. doi:10.1111/j.1551-2916.2006.00991.x

7. Hollenstein E, Davis M, Damjanovic D, Setter N (2005) Appl Phys Lett 87(182905):1
8. Li J-F, Wang K, Zhang B-P, Zhang L-M (2006) J Am Ceram Soc 89:706. doi:10.1111/j.1551-2916.2005.00743.x
9. Wang R, Xie R-J, Hanada K, Matsusaki K, Bando H, Itoh M (2005) Phys Status Solidi 202:R57. doi:10.1002/pssa.200510014
10. Zhang B-P, Li J-F, Wang K, Zhang H (2006) J Am Ceram Soc 89:1605. doi:10.1111/j.1551-2916.2006.00960.x
11. Zang G-Z, Wang J-F, Chen H-C, Su W-B, Wang C-M, Qi P, Ming B-Q, Du J, Zheng L-M, Zhang S, Shrout TR (2006) Appl Phys Lett 88:212908. doi:10.1063/1.2206554
12. R-Marcos F, Ochoa P, Fernandez JF (2007) J Eur Ceram Soc 27:4125. doi:10.1016/j.jeurceramsoc.2007.02.110
13. Skidmore TA, Milne SJ (2007) J Mater Res 22:2265. doi:10.1557/jmr.2007.0281
14. Powder diffraction File No. 32–0822, International Centre for Diffraction Data, Newton Square, PA, 2001
15. Powder diffraction File No. 71–0945, International Centre for Diffraction Data, Newton Square, PA, 2001
16. Bomlai P, Wichianrat P, Muensit S, Milne SJ (2007) J Am Ceram Soc 90:1650. doi:10.1111/j.1551-2916.2007.01629.x
17. Powder diffraction File No. 84–2003 (2001) International Centre for Diffraction Data, Newton Square, PA
18. Powder Diffraction File No. 48–0997 (2001) International Centre for Diffraction Data, Newton Square, PA
19. Wang Y, Damjanovic D, Klein N, Hollenstein E, Setter N (2007) J Am Ceram Soc 90:3485. doi:10.1111/j.1551-2916.2007.01962.x
20. Lin D, Kwok KW, Chan HLW (2007) J Phys D Appl Phys 40:6060